Supporting Information

For

Enhancing electron transport via graphene quantum dot/SnO_2 composites for efficient and durable flexible perovskite photovoltaics

Yu Zhou[1], Sisi Yang[1], Xuewen Yin[1], Jianhua Han[1], Meiqian Tai[1], Xingyue Zhao[1], Hui Chen[2], Youchen Gu[1], Ning Wang[2,3*], Hong Lin[1*]

[1]State Key Laboratory of New Ceramics & Fine Processing, School of Materials Science and Engineering, Tsinghua University, Beijing 100084, China.

[2]State Key Laboratory of Electronic Thin Film and Integrated Devices, University of Electronic Science and Technology of China, Chengdu 610054, China.

[3]State Key Laboratory of Marine Resource Utilization in South China Sea, Hainan University, Haikou 570228, China

**Corresponding E-mail: hong-lin@mail.tsinghua.edu.cn; wangninguestc@gmail.com*

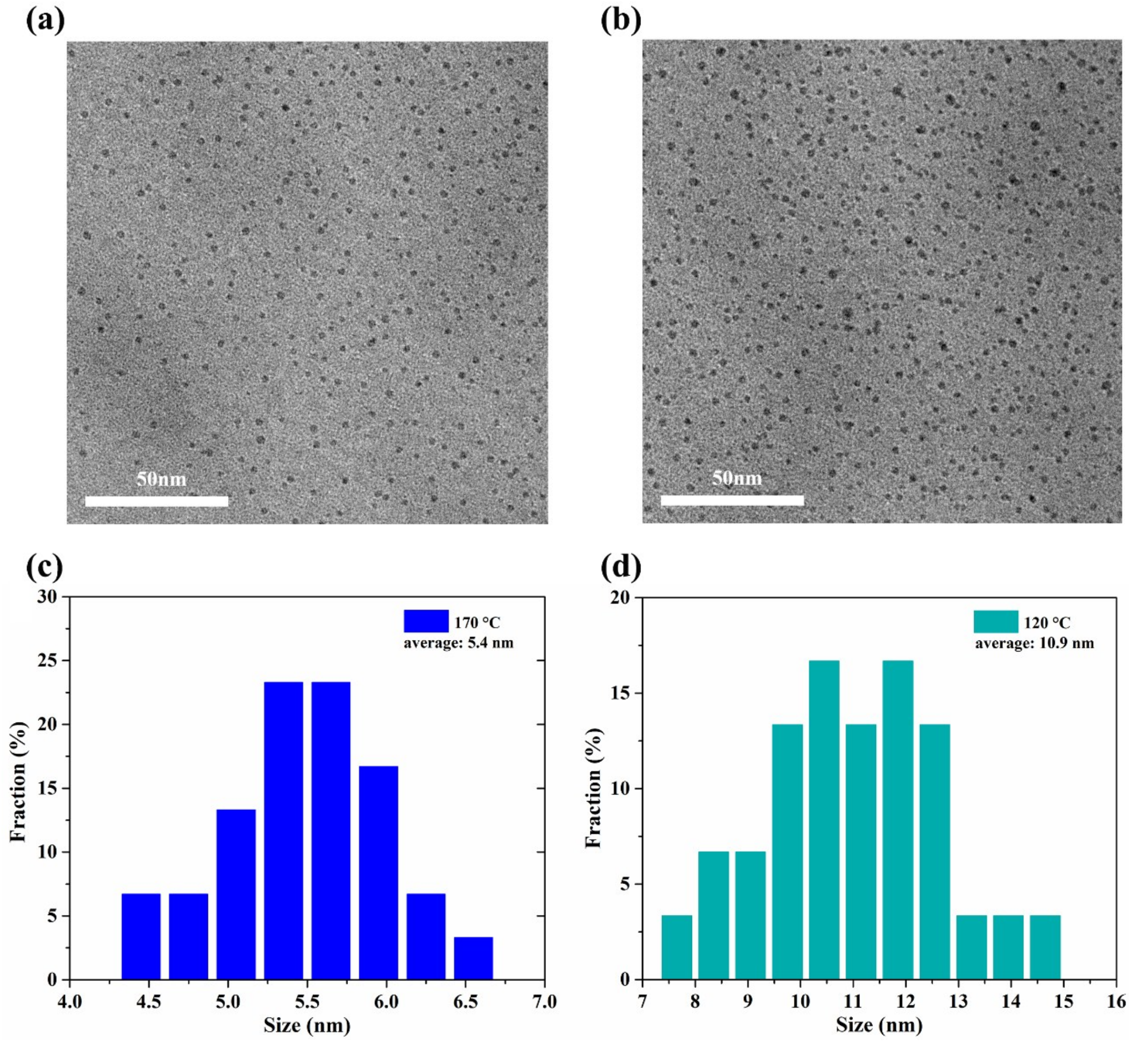

Fig. S1. TEM images of synthesized GQDs. (a) synthesized at 170 °C; (b) synthesized at 120 °C; (c) diameter distribution of GQDs-170 °C; (d) diameter distribution of GQDs-120 °C.

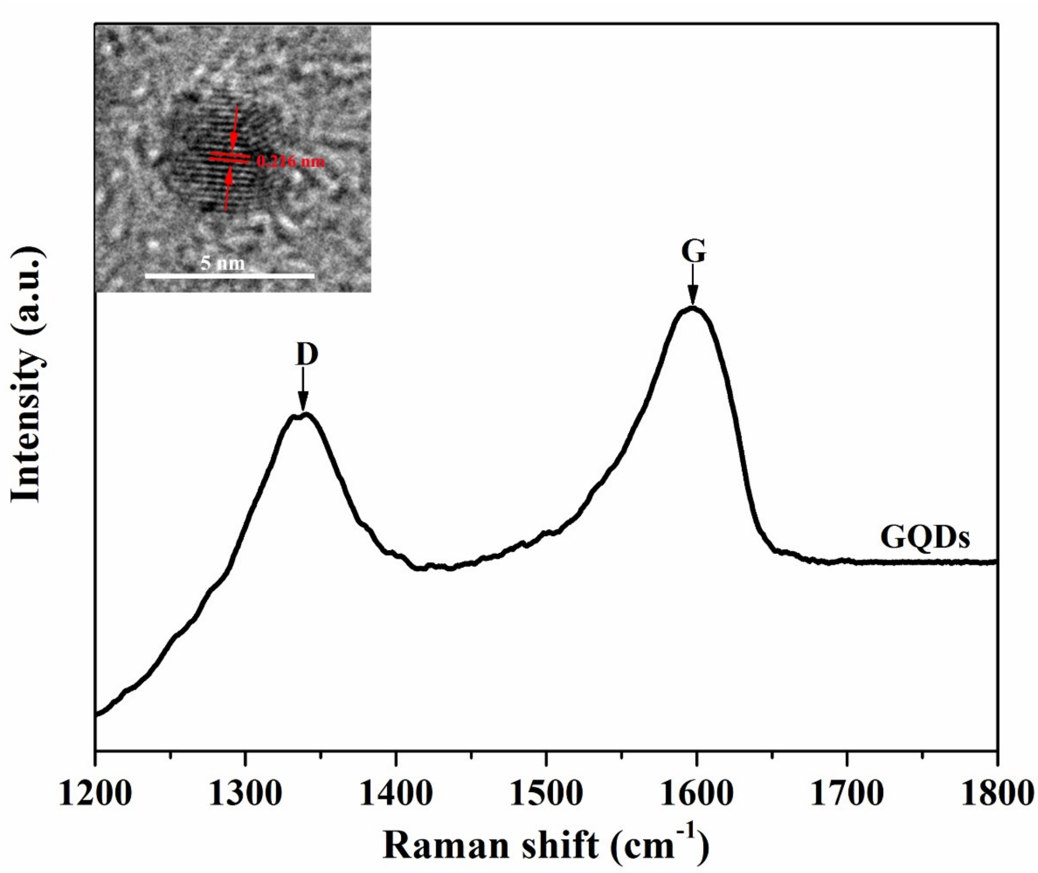

Fig. S2. Raman spectrum of synthesized GQDs. The inset is a single GQD's HRTEM image with marked in-plane lattice space.

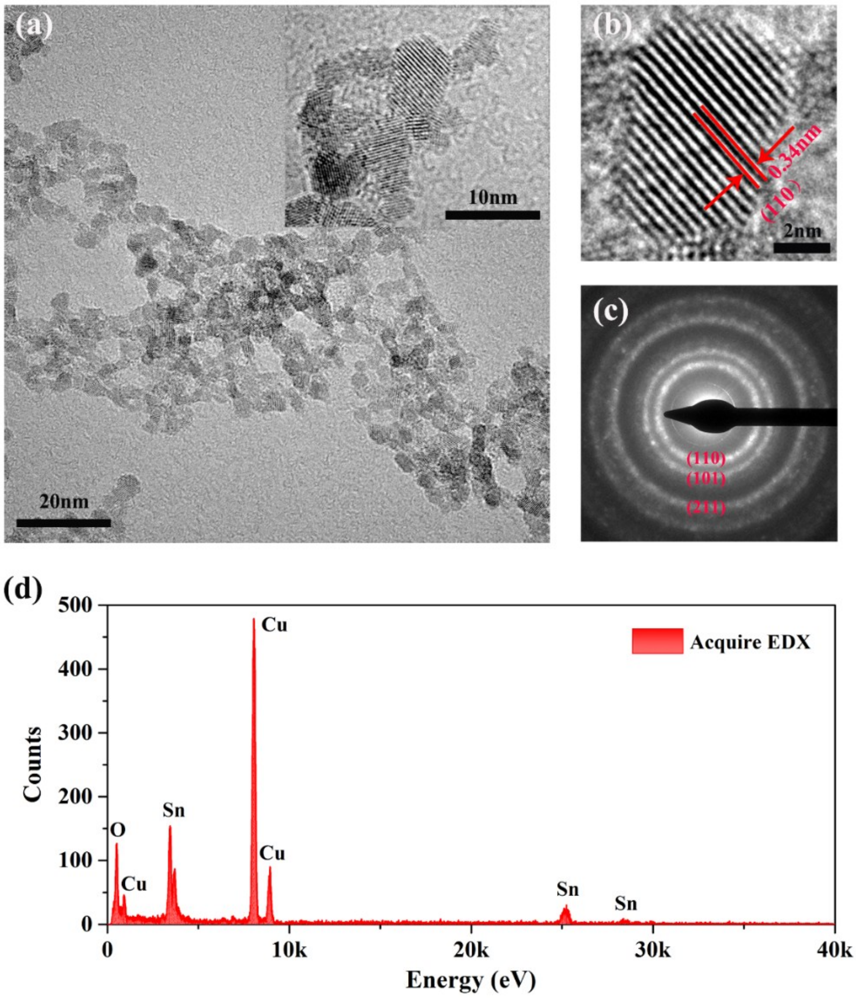

Fig. S3. Properties of SnO_2 nanoparticles: (a) TEM image (inset: image with the scale bar of 10 nm); (b) High-resolution TEM image with marked crystal lattice of the (110) plane; (c) Electron diffraction with observed diffraction circles from the (110), (101) and (211) planes of SnO_2 nanoparticles; (d) EDX spectrum of SnO_2 nanoparticles.

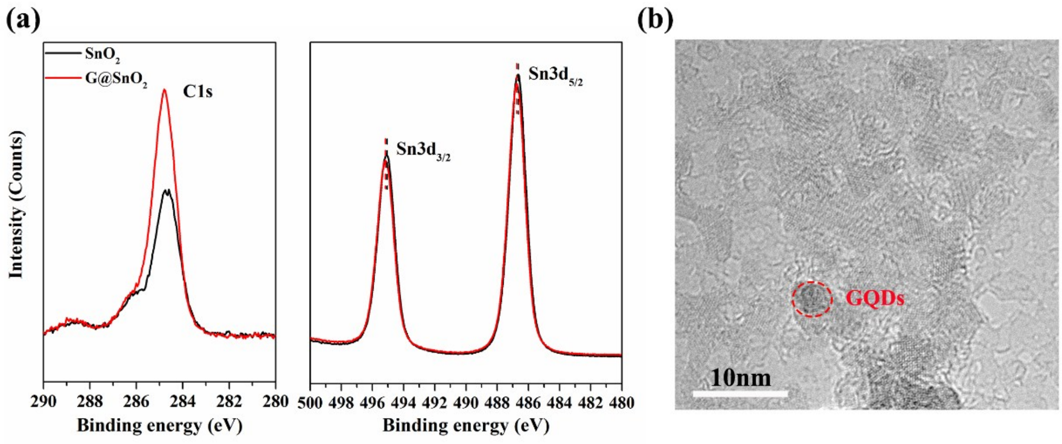

Fig. S4. (a) XPS spectra of C1s and Sn3d of SnO_2 and G@SnO_2. It is obvious that Sn 3d peaks of G@SnO_2 shift to higher binding energy by ~0.10 eV compared to SnO_2; (b) TEM images of SnO_2 nanoparticles mingled with GQDs.

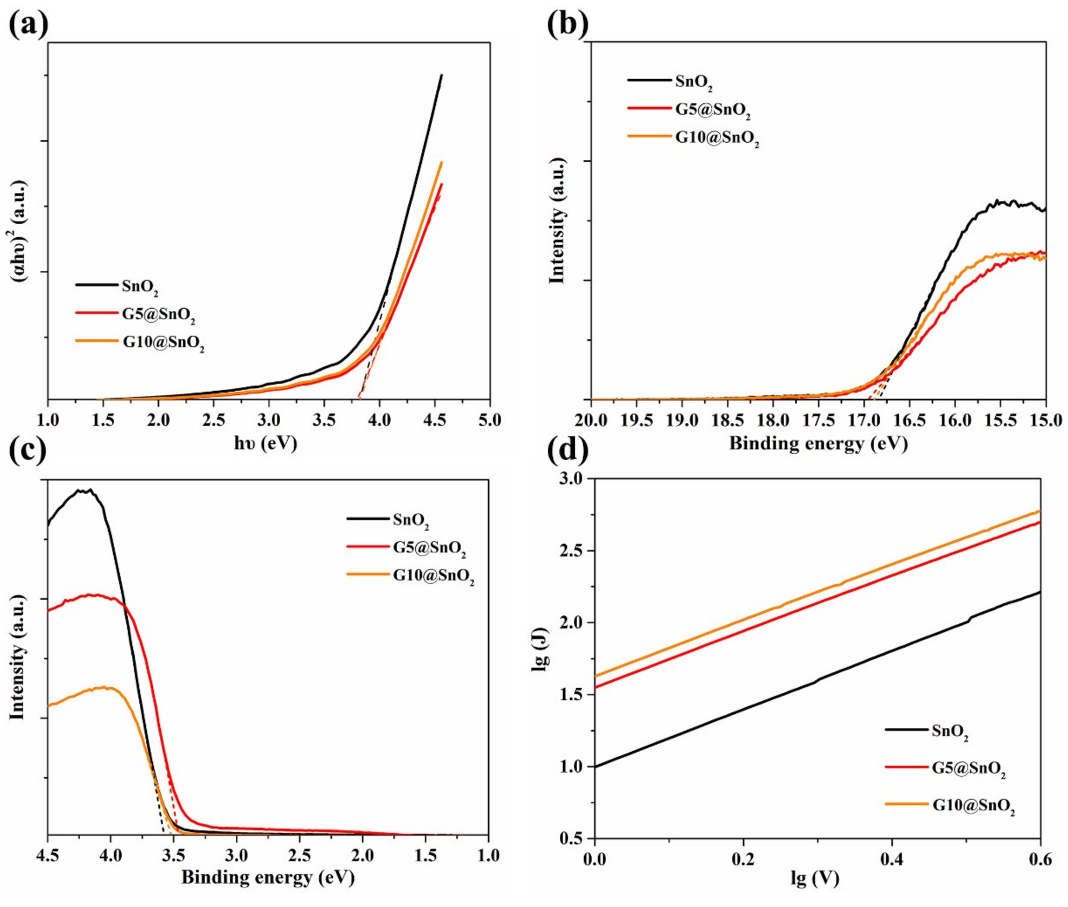

Fig. S5. Band structure properties of different ETLs. (a) Relationship of $(\alpha h\nu)^2$ vs energy; ultraviolet photoelectron spectroscopy (UPS) spectra describing (b) cut-off energy (E_{cutoff}) and (c) Fermi edge (E_{F}, edge); (d) lg(*J*)–lg(*V*) curves using space-charge-limited current (SCLC) model with ETL-only devices for SnO_2, G5@SnO_2, G10@SnO_2, respectively.

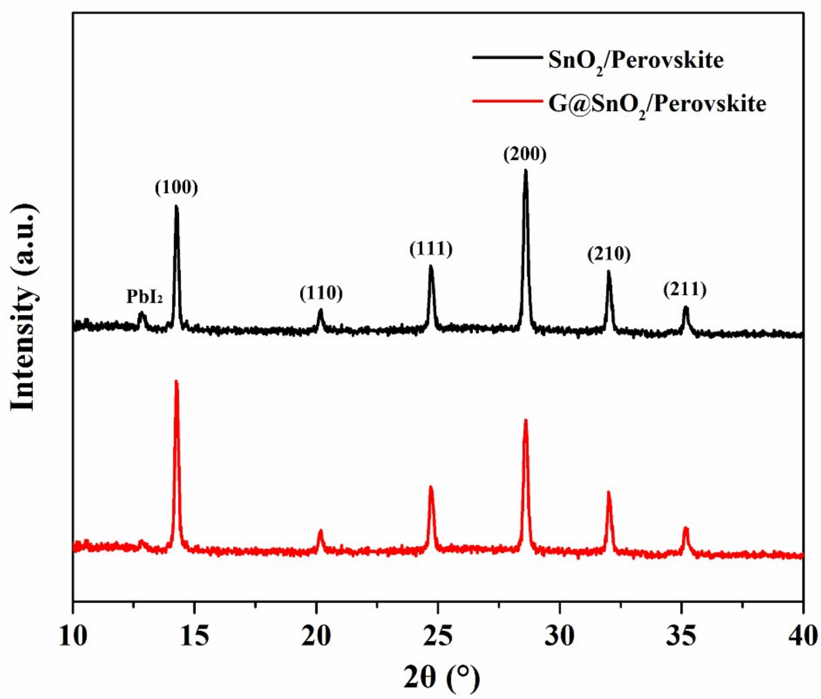

Fig. S6. XRD spectra of mixed perovskite films on pristine SnO_2 and G@SnO_2 substrates.

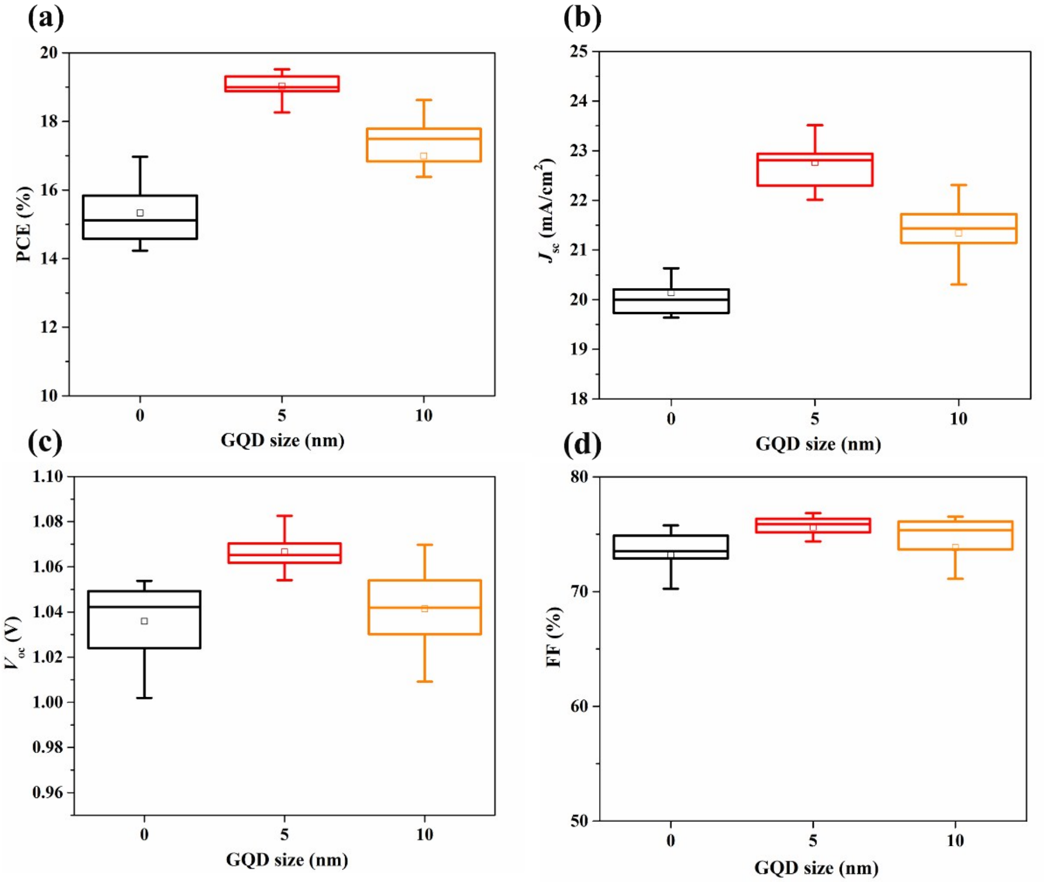

Fig. S7. Photovoltaic parameters of rigid PSCs based on G@SnO_2 ETLs with different GQD sizes: (a) PCE; (b) J_{sc}; (c); V_{oc} (d) FF. Device parameters were collected from 14 devices for each GQD size.

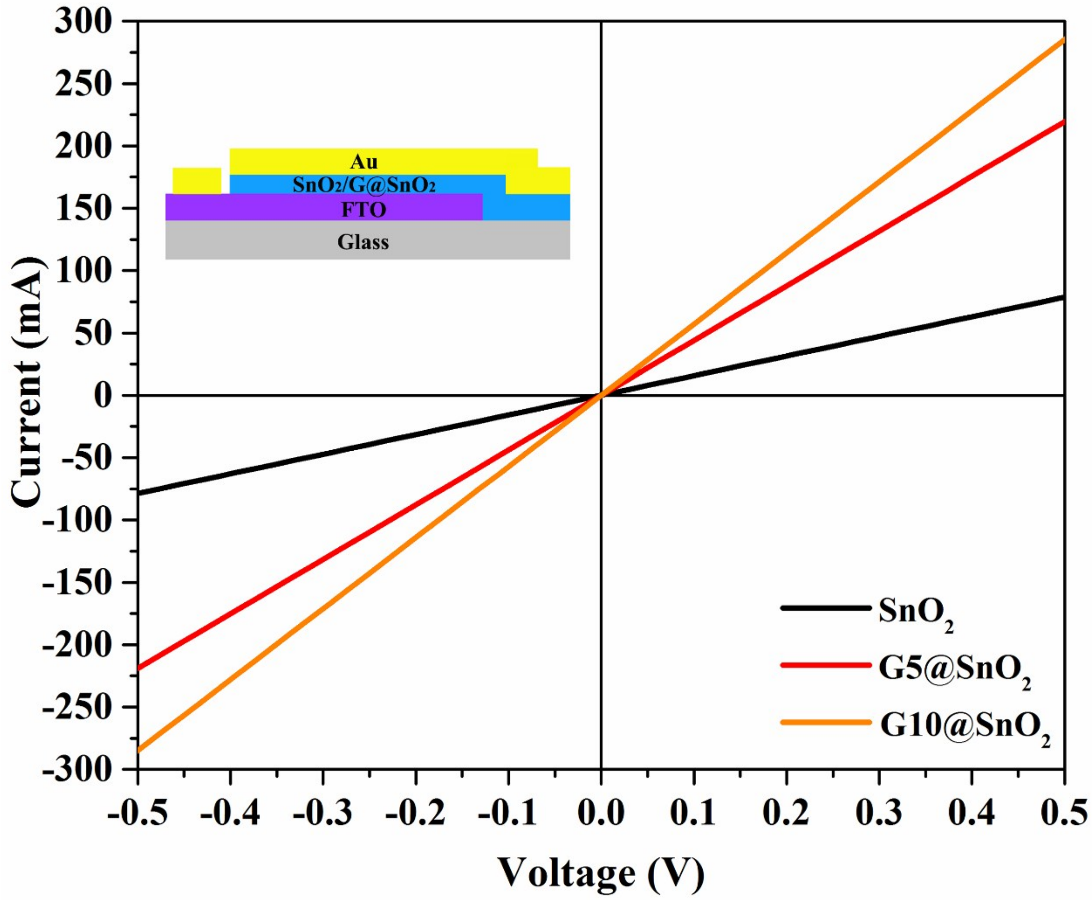

Fig. S8. Linear sweep voltammetry (LSV) curves of FTO/SnO_2/Au (black line), FTO/G5@SnO_2/Au (red line) and FTO/G10@SnO_2/Au (orange line) with an inset of device architecture for LSV measurement

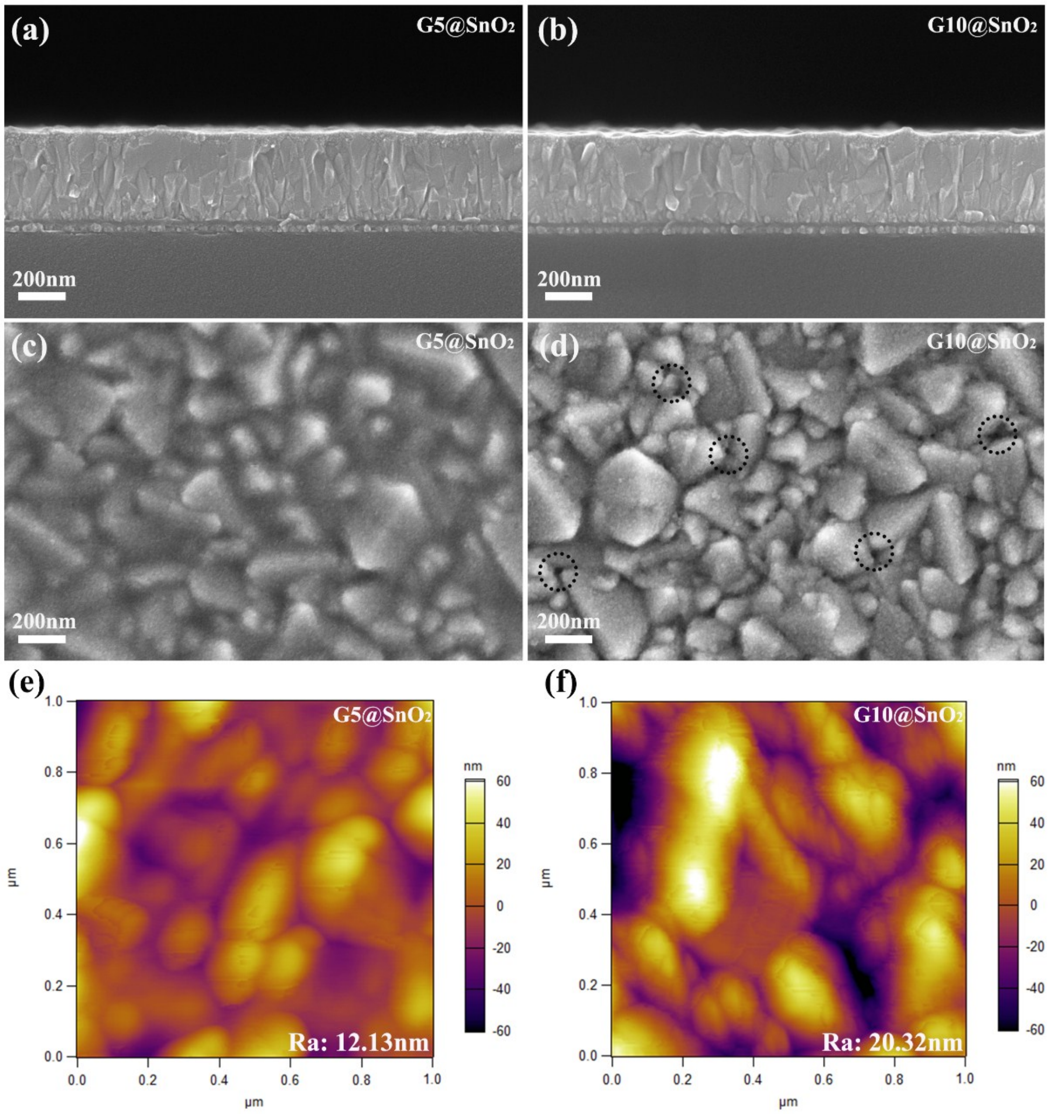

Fig. S9. Cross-sectional SEM images of (a) G5@SnO_2 and (b) G10@SnO_2 on FTO substrates; Top-view SEM images of (c) G5@SnO_2, and (d) G10@SnO_2 on FTO substrates (pinholes were marked by black circles); Surface AFM images of (e) G5@SnO_2, and (f) G10@SnO_2 on FTO substrates.

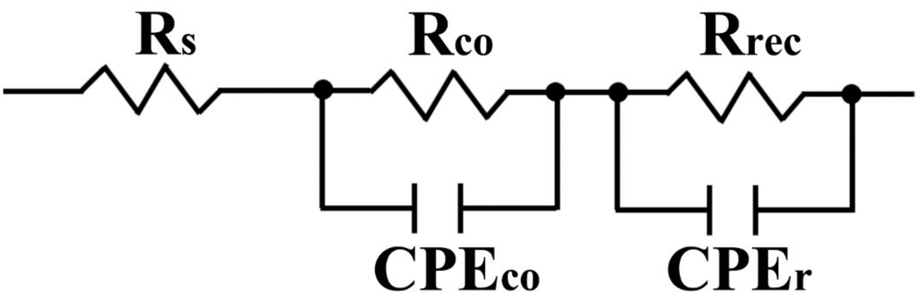

Fig. S10. The equivalent circuit model for PSCs in EIS under dark condition.

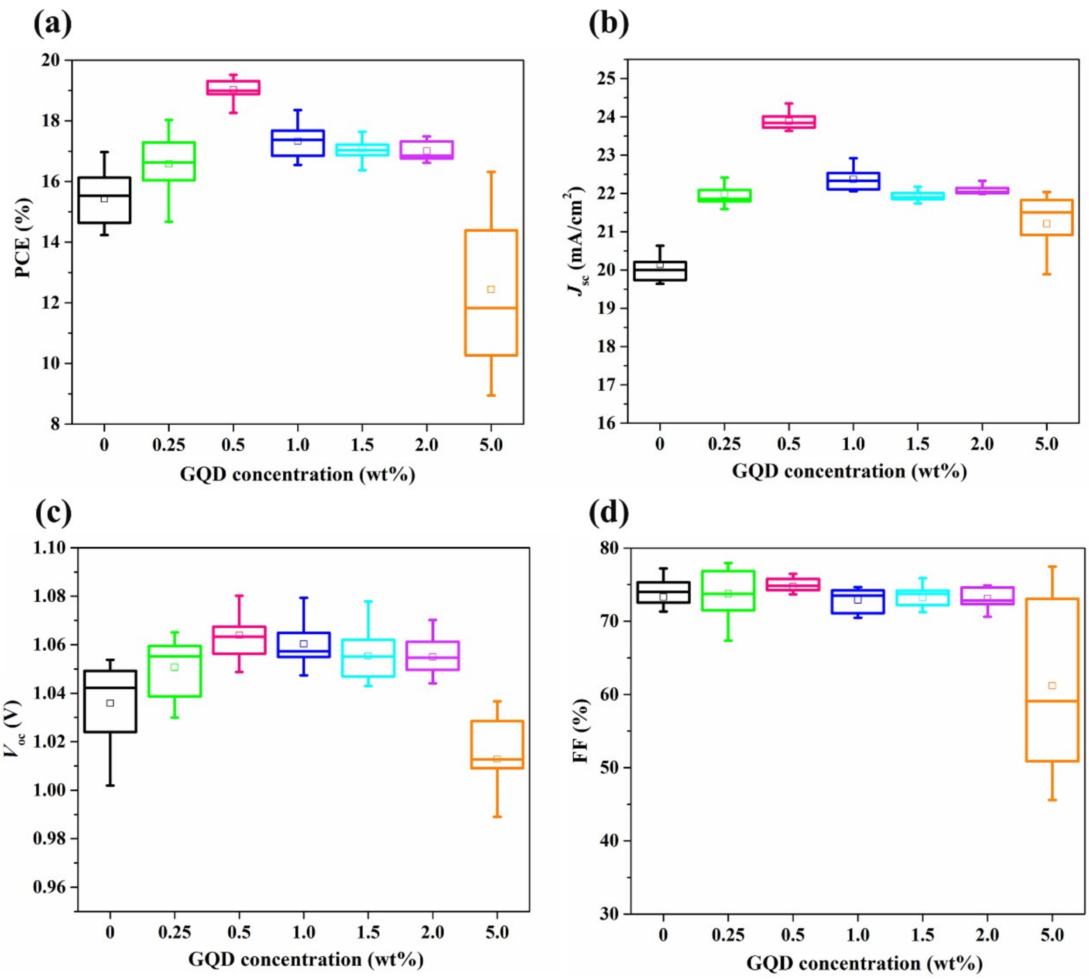

Fig. S11. Photovoltaic parameters of rigid PSCs based on G5@SnO_2 ETLs with different GQD concentrations: (a) PCE; (b) J_{sc}; (c) V_{oc}; (d) FF. The device parameters were collected from 14 devices for each GQD concentration.

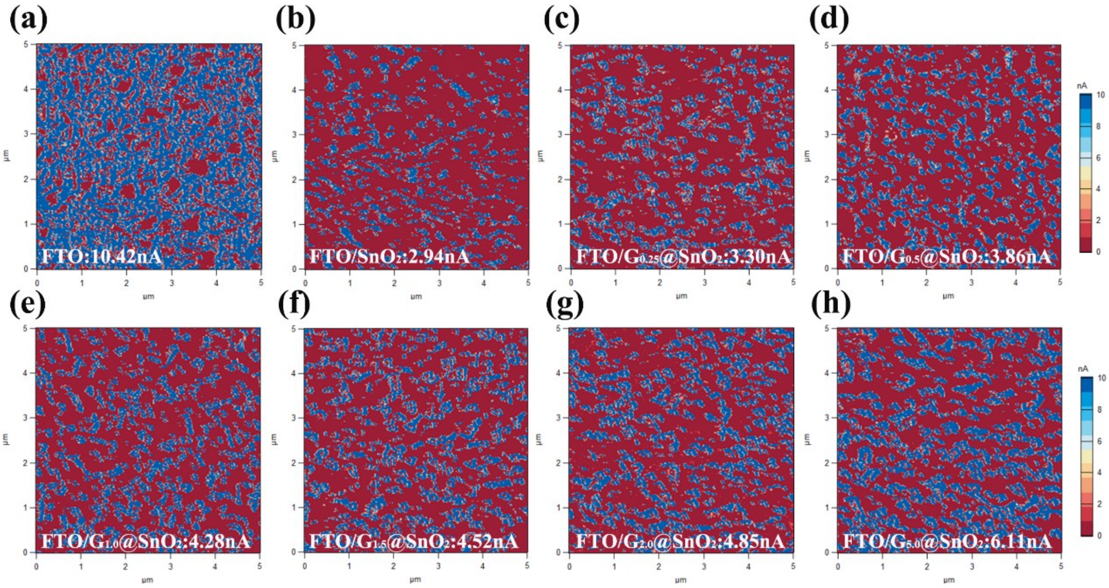

Fig. S12. CAFM images and average detected current values of G5@SnO_2 films on FTO substrates with different GQD concentrations under a bias of 1 V: (a) FTO; (b) 0 wt%; (c) 0.25 wt%; (d) 0.5 wt%; (e) 1.0 wt%; (f) 1.5 wt%; (g) 2.0 wt%; (h) 5.0 wt%. The scale bar represents the current detected by contacted probe in a range of 0 to 10 nA.

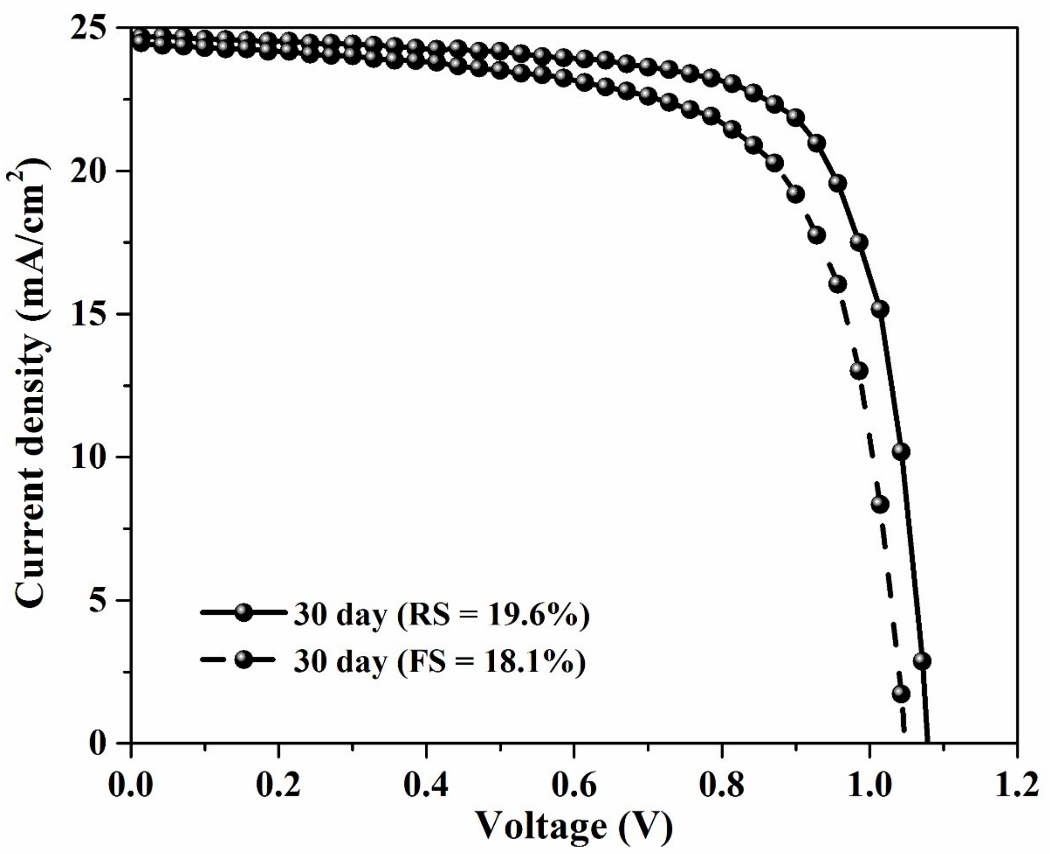

Fig. S13. *J*−*V* curves of the best rigid device with $G_{0.5}5@SnO_2$ ETL after 30-days storing in ambient air (unencapsulated device, T: 25 °C, RH: 25%).

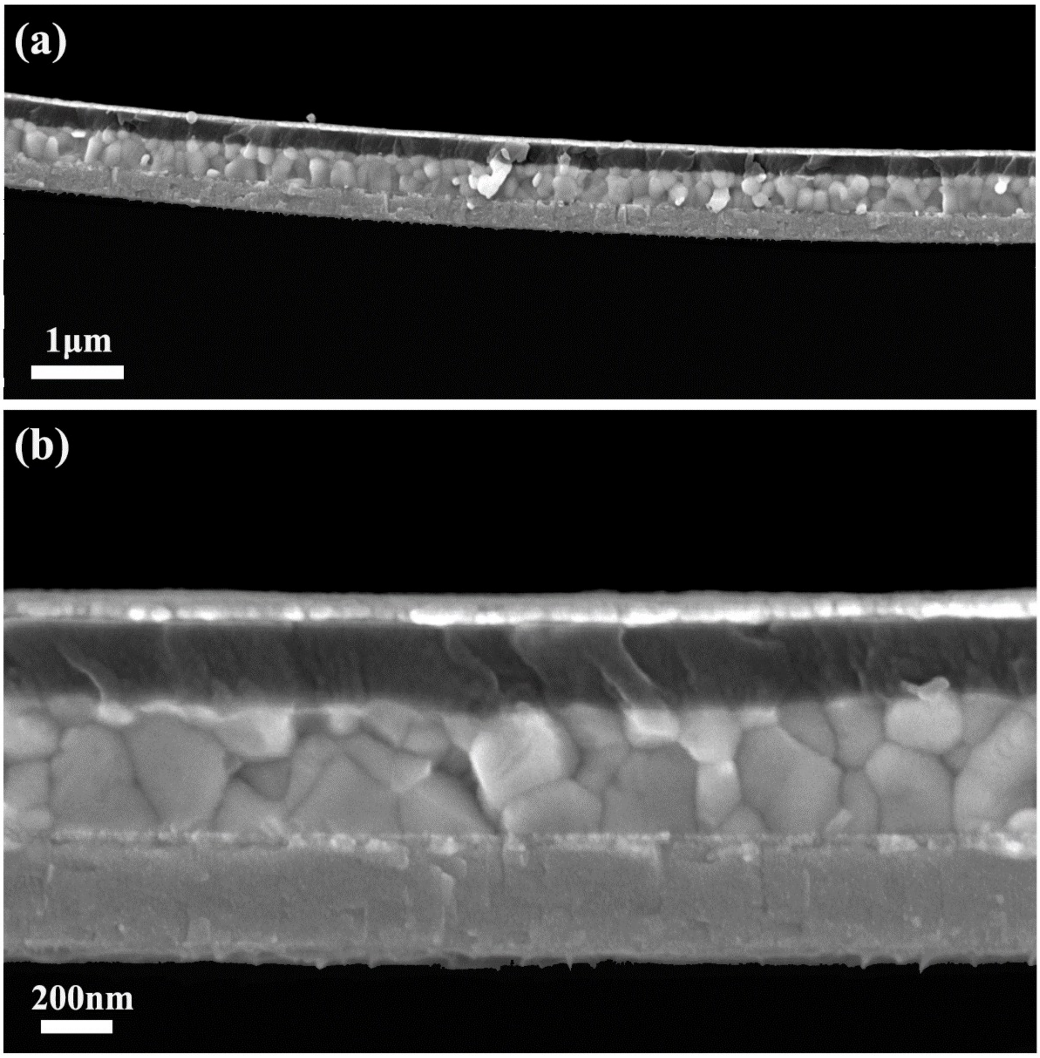

Fig. S14. Cross-sectional SEM images of G5@SnO_2 based flexible perovskite solar cells: (a) large scale size with 1 μm with bending angle; (b) small scale size with 200 nm.

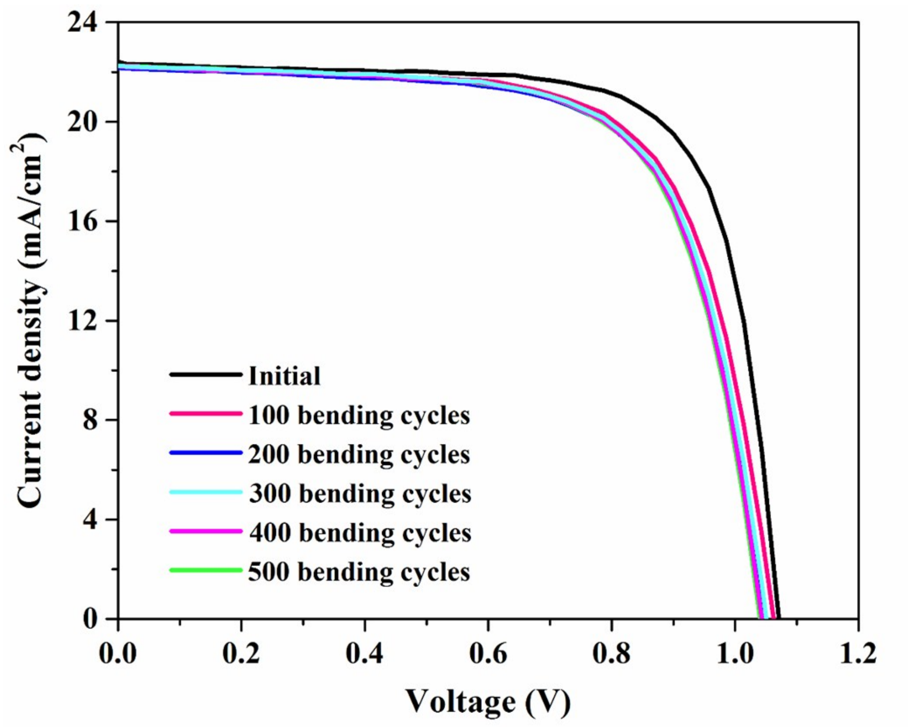

Fig. S15. *J*−*V* curves measured after various bending cycles of flexible PSCs with a bending radius of 7 mm.

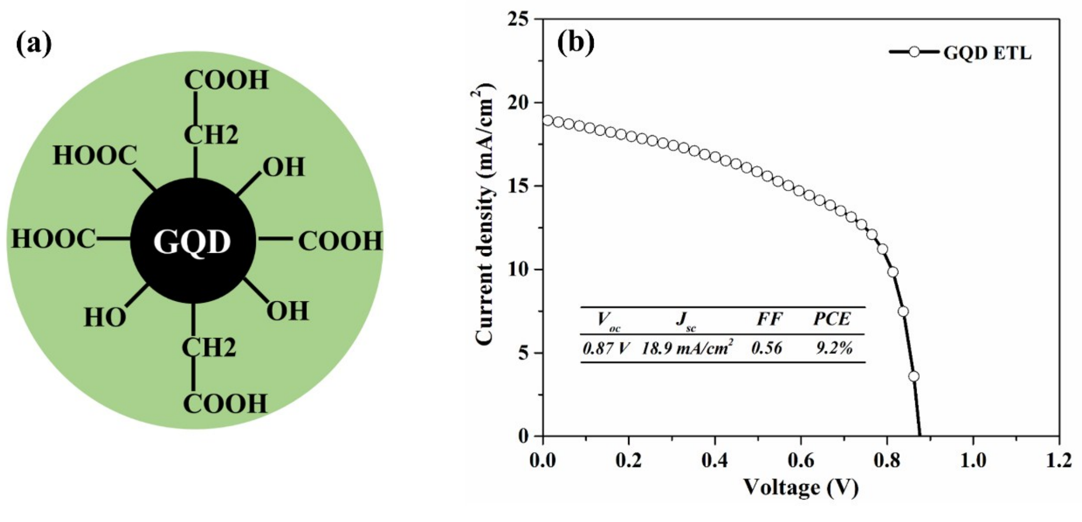

Fig. S16. (a) Schematic diagram of as-synthesized GQD; (b) Best *J*−*V* curve of pure GQD ETL based PSC.

Table S1 Calculated conductivities of SnO_2 and G@SnO_2 ETLs.

ETLs	Slope (I/V)	Thickness (nm)	Conductivity (S/m)
SnO_2	157.11	≈ 30	2.36×10^{-4}
G5@SnO_2	438.20	≈ 30	6.58×10^{-4}
G10@SnO_2	565.28	≈ 30	8.48×10^{-4}

Table S2 Summary of fitted time-resolved photoluminescence spectra of perovskite films based on G@SnO_2 with different sizes of GQD.

Substrates	A_1	τ_1 (ns)	A_2	τ_2 (ns)
Glass	0.35	2.9	0.65	466.5
Glass/SnO_2	0.45	3.6	0.55	402.7
Glass/G5@SnO_2	0.57	2.3	0.43	254.3
Glass/G10@SnO_2	0.46	3.7	0.54	256.5

Table S3 EIS parameters for PSCs under dark condition.

ETLs	R_s (Ω)	R_{rec} (Ω)
SnO_2	15.3	229.0
G5@SnO_2	14.5	357.2
G10@SnO_2	13.4	270.1